Glioblastoma growth modeling for radiotherapy target delineation

Jan Unkelbach[1], Bjoern H. Menze[2], Ali R. Motamedi[1], Florian Dittmann[1], Ender Konukoglu[3], Nicholas Ayache[4], and Helen A. Shih[1]

[1] Massachusetts General Hospital, 30 Fruit Street, Boston, MA 02114, USA
[2] Computer Vision Laboratory, ETH Zürich, Switzerland
[3] Microsoft Research, Cambridge, UK
[4] Asclepios Project, INRIA Sophia Antipolis, France

Abstract. Radiotherapy treatment planning requires a localization of the tumor within the patient. This is challenging to accomplish for microscopic infiltrative spread of disease that is not visible on current imaging modalities. Prime examples for infiltrative tumors are gliomas. With the help of mathematical models, common growth characteristics of gliomas, which are known from histopathological studies, can be incorporated in radiotherapy target delineation. This requires an imaging based personalization of the model to the individual patient. We demonstrate use cases of the Fisher-Kolmogorov glioma growth model in radiotherapy planning of a clinical case. We further analyze the crucial input parameters to the model, in particular, the need for reliable segmentation of anatomical boundaries such as the falx cerebri and the tentorium cerebelli.

Keywords: glioblastoma, radiotherapy planning, target delineation, tumor modeling

1 Introduction

Glioma differ from many solid tumors in the sense that they grow infiltratively. Instead of forming a solid tumor mass with a defined boundary, glioma cells infiltrate the adjacent brain parenchyma. It is well known that tumor cells can be found several centimeters beyond the tumor mass that is visible MRI. Currently, radiotherapy planning is mostly based on the enhancing tumor mass visible on post contrast T1 weighted imaging, as well as the peritumoral edema region visible on T2 weighted images. To account for the infiltrative growth, a 2-3 centimeter wide margin is added to the visible tumor mass to form the clinical target volume (CTV), which is irradiated to a homogeneous dose of 60 Gray. The current treatment planning procedure can potentially be improved by accounting for anisotropic growth patterns of gliomas that are currently not or not consistently incorporated in target delineation. The spatial growth of glioma is influenced by three factors:

1. Anatomical boundaries: The dura, including its extensions falx cerebri and tentorium ceribelli, represents a boundary for migrating tumor cells. Also, except for rare cases of CSF seeding, gliomas do not infiltrate the ventricles.

2. Tumor cells infiltrate gray matter much less than white matter.
3. Tumor cells seem to migrate primarily along white matter fiber tracts.

These macroscopic growth characteristics are partly known from histopathological analysis after autopsy or resection. In parts, these growth patterns are also observed from MR imaging. A comprehensive review can be found in [1].

Incorporating these growth patterns in radiotherapy target volume delineation requires a combination of both mathematical tumor growth modeling and analysis of clinical imaging data. In this work, we use a phenomenological model of tumor growth based on the Fisher-Kolmogorov equation [2–4]. The patient's MRI imaging data is used to personalize the model for application in treatment planning [5–8]. The tumor growth model yields a spatial distribution of infiltrating tumor cells in the brain. This can be used in radiotherapy planning by defining the target volume as an isoline of the tumor cell density [9, 10]. For an application of the model in clinical practice, additional challenges need to be addressed. This includes a characterization of the situations in which the model based target volumes lead to differences compared to manually drawn target volumes. In addition, a sensitivity analysis is needed. The crucial inputs to the model need to be understood and the implications of uncertainty in model inputs and parameters need to be investigated.

In section 2, we briefly summarize the underlying tumor growth model. In section 3 we discuss brain segmentation which turns out to be the most crucial model input. In section 4 we present results and illustrate the use of the model for target delineation. The impact of model parameter choices is discussed.

2 Tumor growth model

2.1 Parameterization of tumor infiltration

It is assumed that two processes describe tumor growth: local proliferation of tumor cells and diffusion of cells into neighboring brain tissue. Mathematically, this is formalized via the Fisher-Kolmogorov equation, a partial differential equation of reaction-diffusion type for the tumor cell density $c(\boldsymbol{r}, t)$ as a function of location $\boldsymbol{r}$ and time t:

$$\frac{\partial}{\partial t} c(\boldsymbol{r}, t) = \nabla \cdot (D(\boldsymbol{r}) \nabla c(\boldsymbol{r}, t)) + \rho c(\boldsymbol{r}, t) \left(1 - c(\boldsymbol{r}, t)\right) \tag{1}$$

where ρ is the proliferation rate which is assumed to be spatially constant, and $D(\boldsymbol{r})$ is the 3×3 diffusion tensor which depends on location $\boldsymbol{r}$. The first term on the right hand side of equation 1 is the diffusion term that models tumor cell migration into neighboring tissue. The second term is a logistic growth term that describes tumor cell proliferation. In this paper, the diffusion tensor is constructed as

$$D(\boldsymbol{r}) = \begin{cases} D_w \cdot I & \boldsymbol{r} \in \text{white matter} \\ D_g \cdot I & \boldsymbol{r} \in \text{gray matter} \end{cases} \tag{2}$$

where I is the 3×3 identity matrix, and D_g and D_w are scaling coefficients for gray and white matter, respectively. At the boundary of brain tissue consisting of white and gray matter we impose no-flux boundary conditions. In summary, the three growth characteristics described in the introduction are reflected in the model as follows:

1. **Anatomical boundaries:** Are handled through no-flux boundary conditions at the boundary to CSF. It is assumed that infiltrating tumor cells are restricted to white and gray matter and do not infiltrate the ventricles or penetrate the dura.
2. **Reduced gray matter infiltration:** Is described via a larger diffusion coefficient in white matter versus gray matter ($D_w/D_g > 1$).
3. **Preferential spread along white matter fiber tracts:** Can be described via an anisotropic diffusion tensor D. Within white matter, the identity matrix I in equation 2 is replaced by a tensor proportional to the water diffusion tensor that is reconstructed from diffusion tensor MR imaging (DTI) [11, 12]. This is however not considered in this paper.

In this paper, we utilize the model to infer the tumor cell density at the time of diagnostic imaging. A naive integration of the model equation 1 is problematic because the initial condition that corresponds to the current tumor appearance on MRI is unknown. We therefore apply a method previously published in [9] that is based on the traveling wave approximation[5].

2.2 Image based model personalization

In order to apply this model for target delineation, the model equation (1) has to be personalized to the individual patient. This process involves two steps: first, a segmentation of the brain, and second, the choice of model parameters.

Segmentation A segmentation of the brain into the three classes white matter, gray matter, and cerebrospinal fluid (CSF) [6] is required in order to solve the model equation based on the individual patient geometry. The brain segmentation is obtained from the structural MR images, including T1, T2, FLAIR and T1 post contrast. Figure 3 shows an example patient discussed in this paper. Figure 3a shows the coronal T1 weighted post contrast image, revealing a contrast enhancing glioblastoma in the right parietal lobe next to the falx. Also the tentorium cerebelli, representing a boundary for migrating tumor cells, is clearly visible. Figure 3b shows the peritumoral edema visible in the axial FLAIR image. The brain segmentation is shown in 3c. The segmentation methods are discussed in more detail in section 3.

[5] For details see [9]. For the results shown in this paper, it is assumed that the boundary of the enhancing tumor mass on the T1 post contrast image corresponds to a tumor cell density of 70%.

[6] Here, we refer to all tissue that is neither white nor gray matter as CSF, ever though more classes for non-brain tissue can be used in the segmentation.

Model parameters In addition, model parameters need to be determined. For this work, the main model parameter is the ratio D_w/D_g of the diffusion coefficients in white and gray matter[7]. Ideally, model parameters are also estimated for an individual patient. For the parameter D_w/D_g this is difficult to accomplish. Hints on reduced gray matter infiltration mainly comes from histopathological analysis [1], which is not available for an individual patient. To a limited degree, the shape of the edematous region visible on the FLAIR image contains information about the microscopic spread of tumor cells. However, the edema is only a surrogate for infiltrative disease. In many cases, the edema region is mostly confined to white matter. It is, however, unclear to what extent this can be seen as evidence for reduced tumor cell infiltration in gray matter, as this may be due to other physiological reasons [1]. In summary, it is commonly believed that $D_w/D_g \gg 1$, but quantification remains difficult. It is therefore important to discuss the implications of parameter uncertainty for radiotherapy target delineation (as addressed in section 4).

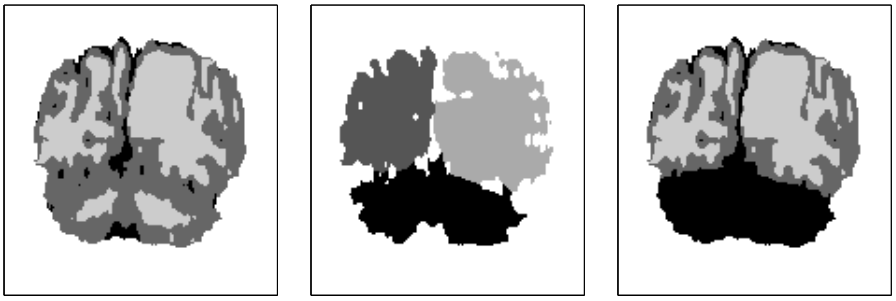

(a) (b) (c)

Fig. 1. (a) EM based brain segmentation into white matter (light gray), gray matter (dark gray), and CSF (black). (b) Segmentation of the cerebral hemispheres and the cerebellum. (c) final segmentation after using the hemisphere segmentation in (b) to remove the cerebellum and separate the hemispheres.

3 Brain segmentation

Modeling the spatial growth of the tumor requires a segmentation of gray matter, white matter, CSF, and non-brain tissue. The normal brain segmentation is primarily based on an Expectation-Maximization (EM) algorithm [13]. The basic component of an EM brain segmentation algorithm can be thought of as

[7] The proliferation rate ρ influences the velocity of tumor growth and how fast the cell density drops with distance from the core [8, 9]. It has however minimal influence on the shape of the tumor, i.e. the spatial shape of the isolines of the tumor cell density (which is the only relevant property in this work).

a gaussian mixture model of the image data. It is assumed that each of white matter, gray matter, and CSF has a characteristic mean image intensity. The actual pixel intensities in the image are assumed to be gaussian distributed around the mean. For segmentation, the class mean values and the class affiliations for every pixel are estimated by maximizing the data likelihood using EM. To favor smooth segmentation boundaries, the basic gaussian mixture model can be augmented by a markov random field regularization term. Here, we adapt out previously published EM based segmentation algorithm, which simultaneously estimates the normal brain segmentation as well as the tumor segmentation on the available sequences [13].

The EM based segmentation algorithm is almost entirely based on gray value information in the image and does not incorporate anatomical information. It yields adequate results for the discrimination of white matter and gray matter. However, it often fails to reliably segment certain anatomical boundaries. This applies in particular to the tentorium cerebelli, an extension of the dura that separates the cerebellum from the cerebral hemispheres. The membrane is thin and consists of only one or two image pixels. In addition, the EM based segmentation may insufficiently separate the cerebral hemispheres through a layer of CSF. This may in particular occur if a tumor mass close to the falx pushes against the membrane. This is illustrated in figure 1, which shows results of the brain segmentation on the coronal slice shown in figure 3a. Figure 1a shows the EM based segmentation. Typically, gray matter and white matter are sufficiently differentiated. However, the algorithm fails to separate the two hemispheres near the tumor mass, and fails to identify the tentorium cerebelli. For a reliable application of the tumor growth model for target delineation, the result of the EM based segmentation has to be enhanced via anatomical information.

Here, we adapt the adaptive disconnection algorithm published by Zhao [14], a method to segment the cerebellum as well as the two cerebral hemispheres. A result of the adaptive disconnection algorithm is shown in figure 1b. This anatomical information is used to amend the EM based segmentation. First, the cerebellum is removed. This is motivated by the fact that supratentorial gliomas almost never infiltrate the cerebellum. In addition, a two pixel thick layer in between the two hemispheres is identified. These pixels are marked as CSF in the final brain segmentation if those pixels were gray matter in the original EM based segmentation. White matter pixels in the EM segmentation are unchanged in order to leave the corpus callosum in tact, which connects the two hemispheres via white matter fiber tracts. The corrected segmentation is shown in figure 1c.

4 Model based target delineation

4.1 Spatial distribution of tumor cells

Figure 2 shows the simulated tumor cell density for three different values of the parameter D_w/D_g on the axial slice shown in figure 3b. For $D_w/D_g = 1$ (figure 2a), the anisotropy in tumor growth is only dependent on anatomical boundaries. In the example shown here, the tumor growth model can be used

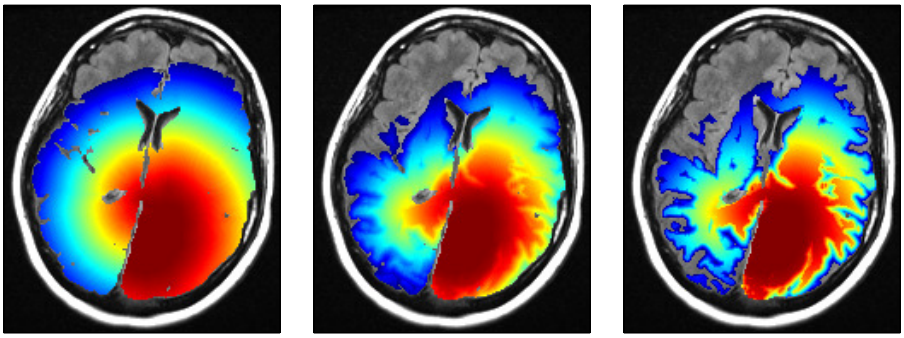

(a) $D_w/D_g = 1$ (b) $D_w/D_g = 10$ (c) $D_w/D_g = 100$

Fig. 2. Simulated tumor cell density on a logarithmic scale for three different values of the parameter D_w/D_g.

to consistently model the complex anatomical conditions created by the falx (representing a boundary) and the corpus callosum (representing a route for tumor cells to spread to the contralateral hemisphere). This is difficult to take into account for in manual target delineation. For $D_w/D_g = 100$ (figure 2c), the tumor cell density follows closely the white matter structure, which can be seen from the comparison to the segmentation in figure 3c. For $D_w/D_g = 10$ (figure 2b) an intermediate result is obtained.

4.2 Target volume definition

For radiotherapy planning, the tumor growth model is used to define the target volume as an isoline of the tumor cell density. This is illustrated in figures 3a and 3b. Shown are the model derived target volumes for the tumor cell densities in figure 2. The contours correspond to the same isoline of the tumor cell density. This isoline was chosen based on the tumor cell density for $D_w/D_g = 1$ such that the size of the model derived target volume matches the size of the manually drawn target volume that was used in the clinically applied treatment plan.

It is apparent that the target volumes for different values of the parameter D_w/D_g are not substantially different, even though the simulated tumor cell densities in figure 2 appear very distinct. The reason for that is the limited thickness of the cortex, i.e. gray matter represents a layer on top of the white matter structure that is only a few millimeters thick. Therefore, reduced infiltration of gray matter has limited influence in the global shape of the target volume. It mainly leads to local changes around the sulci. For large D_w/D_g values, a thin layer of gray matter surrounding the sulci is excluded from the target volume. However, for this patient, this has little impact on radiotherapy planning, because such small volumes cannot be spared from with available irradiation techniques.

Reduced gray matter infiltration may lead to more substantial changes in the target volumes near large accumulations of gray matter. This is, for example, the

case for tumors located closer to the lateral sulcus (Sylvian fissure). In that case, large areas of gray matter are excluded from the target volume for $D_w/D_g = 100$ (results not shown).

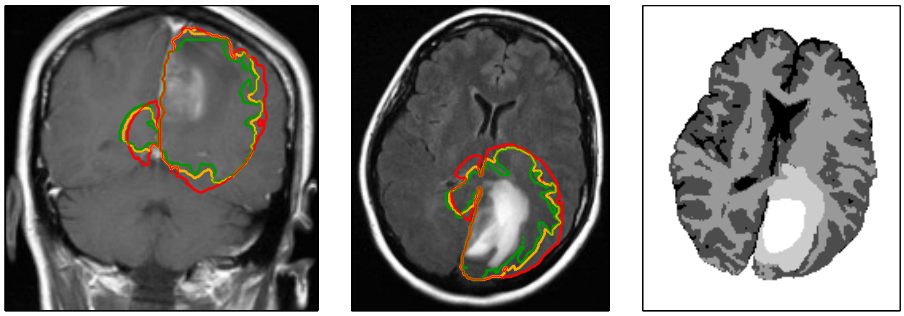

(a) (b) (c)

Fig. 3. Radiographic appearance of a glioblastoma: (a) coronal T1 weighted post contrast image, (b) axial FLAIR image. The three contours show the model derived target volumes discussed in section 4 (red, $D_w/D_g = 1$; yellow, $D_w/D_g = 10$; green, $D_w/D_g = 100$). Figure (c) shows the brain segmentation into CSF, gray matter, white matter, edema, and enhancing core (from black to white).

5 Conclusion

Gliomas show complex spatial growth patterns, which are influenced by anatomical boundaries and the distribution of white and gray matter. These growth characteristics can be formalized using a reaction-diffusion equation. A brain segmentation based on MRI images is used to personalize the tumor growth model. In our work, we aim at bringing this tumor growth model to an application in radiotherapy target delineation. In the first stage, the model can be used to consistently incorporate anatomical boundaries into target delineation. This is in particular useful for tumors located close to the falx and the corpus callosum. This approach only requires a reliable segmentation of the brain. In this paper, this has been achieved via a hybrid approach where an EM based brain segmentation is enhanced by a segmentation of the cerebral hemisphere and the cerebellum. In the next stage, reduced gray matter infiltration can be incorporated. For most parts of the target volume, this has little impact on radiotherapy planning because the cortical thickness is only a few millimeters. However, in regions of major sulci with large accumulations of gray matter, the model can suggest regions where the target volume can be trimmed.

References

1. S. W. Coons. Anatomy and growth patters of diffuse gliomas. In M. S. Berger and C. B. Wilson, editors, *The gliomas*, pages pp 210–225, Philadelphia, PA, USA, 1999. W.B. Saunders Company.
2. Murray J.D. *Mathematical Biology II: Spatial Models and Biomedical Applications*. Springer, 2002.
3. H. L. P. Harpold, E. C. Alvord, and K.R. Swanson. The evolution of mathematical modeling of glioma proliferation and invasion. *J. Neuropathology Exp Neurol*, 66(1):1–9, 2007.
4. E. Mandonnet, J. Pallud, O. Clatz, L. Taillandier, E. Konukoglu, H. Duffau, and L. Capelle. Computational modeling of the WHO grade II glioma dynamics: principles and applications to management paradigm. *Neurosurg Rev*, 31(3):263–269, Jul 2008.
5. E.D. Angelini, O. Clatz, E. Mandonnet, E. Konukoglu, L. Capelle, and H. Duffau. Glioma dynamics and computational models: a review of segmentation, registration, and in silico growth algorithms and their clinical applications. *Current Medical Imaging Reviews*, 3(4):262–276, 2007.
6. N. C. Atuegwu, J. C. Gore, and T. E. Yankeelov. The integration of quantitative multi-modality imaging data into mathematical models of tumors. *Phys Med Biol*, 55(9):2429–2449, May 2010.
7. Bjoern H. Menze, Koen Van Leemput, Antti Honkela, Ender Konukoglu, Marc-Andr Weber, Nicholas Ayache, and Polina Golland. A generative approach for image-based modeling of tumor growth. *Inf Process Med Imaging*, 22:735–747, 2011.
8. Ender Konukoglu, Olivier Clatz, Bjoern H. Menze, Bram Stieltjes, Marc-Andr Weber, Emmanuel Mandonnet, Herve Delingette, and Nicholas Ayache. Image guided personalization of reaction-diffusion type tumor growth models using modified anisotropic eikonal equations. *IEEE Trans. Med. Imaging*, 29(1):77–95, 2010.
9. Ender Konukoglu, Olivier Clatz, Pierre-Yves Bondiau, Herve Delingette, and Nicholas Ayache. Extrapolating glioma invasion margin in brain magnetic resonance images: Suggesting new irradiation margins. *Medical Image Analysis*, 14:111–125, 2010.
10. D. Cobzas, P. Mosayebi, A. Murtha, and M. Jagersand. Tumor invasion margin on a riemannian space of brain fibers. In *LNCS 5762 Proc. MICCAI Part 2*, pages pp 531–39, Heidelberg, Germany, 2009. Springer.
11. O. Clatz, M. Sermesant, P. Y. Bondiau, H. Delingette, S. K. Warfield, G. Malandain, and N. Ayache. Realistic simulation of the 3-D growth of brain tumors in MR images coupling diffusion with biomechanical deformation. *IEEE Trans Med Imaging*, 24(10):1334–1346, Oct 2005.
12. Sad Jbabdi, Emmanuel Mandonnet, Hugues Duffau, Laurent Capelle, Kristin Rae Swanson, Mlanie Plgrini-Issac, Rmy Guillevin, and Habib Benali. Simulation of anisotropic growth of low-grade gliomas using diffusion tensor imaging. *Magnetic Resonance in Medicine*, 54(3):616–624, 2005.
13. B. Menze, K. Van Leemput, D. Lashkari, M. Weber, N. Ayache, and P. Golland. A generative model for brain tumor segmentation in multi-modal images. In *Proc MICCAI*, Heidelberg, 2010. Springer.
14. Lu Zhao, Ulla Ruotsalainen, Jussi Hirvonen, Jarmo Hietala, and Jussi Tohka. Automatic cerebral and cerebellar hemisphere segmentation in 3d mri: Adaptive disconnection algorithm. *Medical Image Analysis*, 14(3):360–372, 2010.